Proc. Natl. Acad. Sci. USA
Vol. 77, No. 6, pp. 3186–3190, June 1980
Biochemistry

Theoretical model for the cooperative equilibrium binding of myosin subfragment 1 to the actin–troponin–tropomyosin complex

(calcium binding/neighbor interactions/cooperativity/Ising model/grand partition function)

TERRELL L. HILL*, EVAN EISENBERG†, AND LOIS GREENE†

*Laboratory of Molecular Biology, National Institute of Arthritis, Metabolism and Digestive Diseases and †Laboratory of Cell Biology, National Heart, Lung, and Blood Institute, National Institutes of Health, Bethesda, Maryland 20205

Contributed by Terrell L. Hill, February 25, 1980

ABSTRACT **Recent experimental data on the equilibrium binding of myosin subfragment 1 (S-1) to regulated actin filaments in the presence and in the absence of Ca^{2+} are analyzed by using a linear Ising model. In the model, each tropomyosin–troponin unit (including seven sites on the actin filament) can be in one of two possible states, which have different intrinsic free energies and different binding constants for S-1. Bound S-1 molecules do not interact with each other. There are nearest-neighbor (pair) interactions between these units that depend on the state of each member of the pair and on the number of Ca^{2+} bound to one member of the pair. There are two sources of positive cooperativity in this system: the fact that seven actin sites change state together as part of a single unit; and the existence of attractive nearest-neighbor interactions between units. Parameters in the model are evaluated by fitting the data, both in the presence and in the absence of Ca^{2+}. Several extensions of this model are discussed.**

In a recent paper, Greene and Eisenberg (1) presented experimental data on the equilibrium binding of the myosin-subfragment-1–ADP complex (hereafter simply referred to as S-1, for brevity) to the troponin–tropomyosin–F-actin complex (regulated F-actin), in the presence and in the absence of Ca^{2+}. The binding isotherms show interesting cooperativity (the data are included in Fig. 2, below). A tentative interpretation and analysis of the data were given (1) based on a simple model (ref. 2, equations 10–12a with $\tau = 0$; ref. 3, equations 7-70 and 7-71 with $\tau = 0$) that does not include nearest-neighbor cooperativity in a quantitative way (see the discussion of Eqs. **22–25**, below). Essentially the same model (in the $\tau = 0$ case), with equivalent equations, was used later by Monod *et al.* (4) to account for the allosteric behavior of regulatory proteins. It is the purpose of the present paper to reinterpret the same data in terms of a more refined model that includes nearest-neighbor interactions between troponin–tropomyosin units on the F-actin.

We are extending the approach of the present paper to the *in vitro* and *in vivo* steady-state ATPase activity of regulated actomysin; this steady-state system serves as a good illustration of recent general theoretical studies (5–9) on the effect of nearest-neighbor interactions on steady-state enzyme behavior.

THE ASSUMED MODEL AND ITS ANALYSIS

We consider a very long actin filament saturated with troponin–tropomyosin, as indicated schematically in Fig. 1*b*. We are interested in the equilibrium binding of S-1 and of Ca^{2+} (Fig. 1*a*) as influenced by each other and by tropomyosin (the troponin is now always understood to be included). Each tropomyosin unit, including seven actin sites for S-1 binding, can be in one of two states: state 1, with "weak" binding (constant K_1) of S-1 on each of the seven actin sites; and state 2 with "strong" binding (constant K_2) of S-1. The bound S-1 molecules do not interact with each other. The *intrinsic* equilibrium constant for $2 \rightleftarrows 1$ in a hypothetical *isolated* tropomyosin unit, with no tropomyosin neighbors and with no bound S-1 or Ca^{2+}, is L, which favors state 1 (weak) over state 2 (strong) ($L > 1$). Each troponin has two equivalent binding sites for Ca^{2+} (the regulatory sites), with intrinsic binding constants K_a and K_b (in states 1 and 2, respectively). The interactions between nearest-neighbor tropomyosin molecules are of types 11, 12, 21, and 22 (Fig. 1*b*). These boundary interactions are modulated by the extent of Ca^{2+} binding (0, 1, or 2) on the two Ca^{2+} sites of the *right-hand* member (Fig. 1*b*) of each nearest-neighbor pair (because of proximity of the right-hand troponin to the pair boundary).

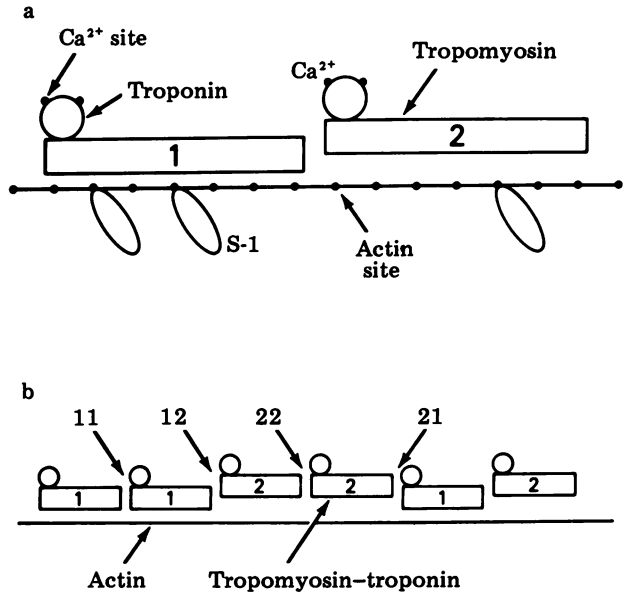

FIG. 1. (*a*) Schematic representation of the two states of the tropomyosin–troponin unit (including seven actin sites). Each troponin has two "regulatory" sites for Ca^{2+}. (*b*) Illustration of the four types of nearest-neighbor pairs in a sequence of units.

State 1 is favored at low S-1 concentrations ($L > 1$). But state 2 dominates at high S-1 concentrations because $K_2 \gg K_1$. The transition from state 1 to state 2 is cooperative for two reasons: because seven actin sites in a unit change state as a group; and, more importantly, because of the nearest-neighbor interactions between units.

The above describes the model qualitatively. This is an es-

The publication costs of this article were defrayed in part by page charge payment. This article must therefore be hereby marked "*advertisement*" in accordance with 18 U. S. C. §1734 solely to indicate this fact.

Abbreviations: HMM, heavy meromyosin; S-1, subfragment 1 of heavy meromyosin; EGTA, ethylene glycol bis(β-aminoethyl ether)-*N,N,N',N'*-tetraacetic acid.

sentially infinite one-dimensional Ising problem, with complications owing to S-1 and Ca^{2+} binding, which can be solved easily and exactly by the matrix method (10–12). Closely related problems, with a ligand-shifted equilibrium and cooperativity, have been treated elsewhere (2, 6). Two generalizations of the above model are discussed in later sections: (*i*) the extent of Ca^{2+} binding also modulates K_1 and K_2; and (*ii*) heavy meromyosin (HMM), two-headed binding only, is the ligand in place of S-1. A third possible generalization, which we do not include here, is to allow variable rather than saturated tropomyosin binding. Other generalizations currently being studied are a continuum of states for each unit and a relaxation of the seven-sites-as-a-unit assumption.

In applying the matrix method (10–12) to this problem, the 2×2 matrix is

$$\begin{pmatrix} \xi_1 Y_{11} & \xi_1 Y_{12} \\ \xi_2 Y_{21} & \xi_2 Y_{22} \end{pmatrix}. \quad [1]$$

The rows here refer to states 1 and 2 of the kth tropomyosin in the chain and the columns refer to states 1 and 2 of the $k+1$th tropomyosin. Also, in Eq. **1**,

$$Y_{11} \equiv x_{11} + 2K_a\rho y_{11} + K_a^2\rho^2 z_{11}, \quad Y_{12} \equiv x_{12} + 2K_b\rho y_{12} + K_b^2\rho^2 z_{12}$$
$$Y_{21} \equiv x_{21} + 2K_a\rho y_{21} + K_a^2\rho^2 z_{21}, \quad Y_{22} \equiv x_{22} + 2K_b\rho y_{22} + K_b^2\rho^2 z_{22} \quad [2]$$

$$\xi_1 \equiv L(1 + K_1c)^7, \; \xi_2 \equiv (1 + K_2c)^7, \quad [3]$$

where c is the concentration of free S-1, ρ is the concentration of free Ca^{2+}, and x_{ij}, y_{ij}, z_{ij} are nearest-neighbor tropomyosin interaction parameters. For example, $x_{21} \equiv e^{-w_{21}/kT}$, where w_{21} is the 21 interaction free energy with no Ca^{2+} bound on the *right-hand* member (in state 1) of the pair, and y_{21}, z_{21} are corresponding parameters for a 21 pair with one and two Ca^{2+} bound, respectively. Incidentally, if two bound Ca^{2+} interact with each other, this effect can be included in the z_{ij}. All degrees of S-1 binding are automatically taken care of by ξ_1 and ξ_2 (3); all factors in Eq. **1** have the form of subsystem grand partition functions (3). The appropriateness of Eq. **1** can be verified by starting with the equivalent but more detailed 6×6 matrix (11, 12) for the six substates 1, 2 (tropo) × 0, 1, 2 (Ca^{2+}):

$$\begin{pmatrix} \xi_1 x_{11} & \xi_1 y_{11} & \xi_1 z_{11} \\ 2\xi_1 K_a\rho x_{11} & 2\xi_1 K_a\rho y_{11} & 2\xi_1 K_a\rho z_{11} \\ \xi_1 K_a^2\rho^2 x_{11} & \xi_1 K_a^2\rho^2 y_{11} & \xi_1 K_a^2\rho^2 z_{11} \\ \xi_2 x_{21} & \xi_2 y_{21} & \xi_2 z_{21} \\ 2\xi_2 K_b\rho x_{21} & 2\xi_2 K_b\rho y_{21} & 2\xi_2 K_b\rho z_{21} \\ \xi_2 K_b^2\rho^2 x_{21} & \xi_2 K_b^2\rho^2 y_{21} & \xi_2 K_b^2\rho^2 z_{21} \end{pmatrix}$$

Again, the rows refer to subunit k and the columns, to $k+1$. The order of states in both cases is 1(0, 1, 2), 2(0, 1, 2). Both S-1 and Ca^{2+} binding factors are assigned to k.

Let γ_m be the larger eigenvalue of the 2×2 matrix in Eq. **1**, let $0 \le \theta \le 1$ be the fraction of actin sites occupied by S-1 molecules, and let $0 \le \sigma \le 2$ be the mean number of Ca^{2+} bound per tropomyosin. Then (3, 11, 12)

$$7\theta = \partial \ln \gamma_m / \partial \ln c, \; \sigma = \partial \ln \gamma_m / \partial \ln \rho \quad [4]$$

$$2\gamma_m = a_1 + a_2 + [(a_1 - a_2)^2 + 4a_1a_2Y^{-1}]^{1/2}, \quad [5]$$

where

$$a_1 \equiv \xi_1 Y_{11}, \; a_2 \equiv \xi_2 Y_{22}, \; Y(\rho) \equiv Y_{11}Y_{22}/Y_{12}Y_{21}. \quad [6]$$

We find from Eqs. **4** and **5**, for θ and σ as functions of c and ρ,

$$\theta = p_1\theta_1 + p_2\theta_2 \quad [7]$$

$$\sigma = p_{11}\sigma_{11} + p_{12}\sigma_{12} + p_{21}\sigma_{21} + p_{22}\sigma_{22}, \quad [8]$$

where p_1 is the fraction of tropomyosin units in state 1, θ_1 is the fraction of state 1 actin sites occupied by S-1, σ_{12} is the mean number of Ca^{2+} bound at a 12 boundary (right-hand tropomyosin, in state 2), p_{12} is the fraction of all nearest-neighbor pairs that are of type 12, etc. Conservation relationships are

$$p_1 + p_2 = 1, \; p_{12} = p_{21}, \; p_{11} + p_{22} + 2p_{12} = 1$$
$$p_1 = p_{11} + p_{12}, \; p_2 = p_{22} + p_{12}. \quad [9]$$

Explicit expressions (6) are

$$\theta_i = K_ic/(1 + K_ic) \quad (i = 1,2)$$
$$\sigma_{ij} = \partial \ln Y_{ij}/\partial \ln \rho \quad (i,j = 1,2) \quad [10]$$

$$\sigma_{11} = 2(K_a\rho y_{11} + K_a^2\rho^2 z_{11})/Y_{11}, \text{ etc.} \quad [11]$$

$$p_2 = 2aY^{-1}/\sqrt{\;}(1 - a + \sqrt{\;}) \quad [12]$$

$$p_{11} = (1 - a + \sqrt{\;})/\sqrt{\;}(1 + a + \sqrt{\;}) \quad [13]$$

$$p_{22} = a(a - 1 + \sqrt{\;})/\sqrt{\;}(1 + a + \sqrt{\;}) \quad [14]$$

$$p_{12} = p_{21} = 2aY^{-1}/\sqrt{\;}(1 + a + \sqrt{\;}), \quad [15]$$

where

$$a \equiv a_2/a_1, \; \sqrt{\;} \equiv [(1 - a)^2 + 4aY^{-1}]^{1/2}. \quad [16]$$

$Y > 1$ introduces positive cooperativity beyond the seven-actin-site effect (Eq. 3). The midpoint of the transition between states 1 and 2 ($p_2 = \frac{1}{2}$) occurs when $a = 1$ (Eq. **12**) for any Y. We cannot expect the usual symmetry of binding isotherm curves in simple Ising models (3) because here $K_1 \neq K_2$ and $K_a \neq K_b$.

The physical significance of

$$a \equiv a_2/a_1 = (1 + K_2c)^7 Y_{22}(\rho)/L(1 + K_1c)^7 Y_{11}(\rho) \quad [17]$$

is that this is the equilibrium constant, *per tropomyosin* unit, for the transition $1 \rightleftarrows 2$ between a filament with all units in state 1 and a filament with all units in state 2, at arbitrary concentrations of S-1 (c) and Ca^{2+} (ρ). $L > 1$ favors state 1; large c favors state 2 ($K_2 \gg K_1$); ρ affects a by altering both the extent of Ca^{2+} binding and the effective nearest-neighbor interaction between 11 and 22 pairs in the two filaments (see Eqs. **2**).

$$\begin{pmatrix} \xi_1 x_{12} & \xi_1 y_{12} & \xi_1 z_{12} \\ 2\xi_1 K_a\rho x_{12} & 2\xi_1 K_a\rho y_{12} & 2\xi_1 K_a\rho z_{12} \\ \xi_1 K_a^2\rho^2 x_{12} & \xi_1 K_a^2\rho^2 y_{12} & \xi_1 K_a^2\rho^2 z_{12} \\ \xi_2 x_{22} & \xi_2 y_{22} & \xi_2 z_{22} \\ 2\xi_2 K_b\rho x_{22} & 2\xi_2 K_b\rho y_{22} & 2\xi_2 K_b\rho z_{22} \\ \xi_2 K_b^2\rho^2 x_{22} & \xi_2 K_b^2\rho^2 y_{22} & \xi_2 K_b^2\rho^2 z_{22} \end{pmatrix}.$$

If we examine an S-shaped experimental $\theta(c)$ (S-1 binding) curve, at fixed ρ, the point at which $a = 1$, $p_2 = \frac{1}{2}$ occurs can be located approximately at the inflection in the curve. Let θ' and c' be the coordinates of this point. Because of the steepness of the experimental curve, c' can be estimated relatively accurately. If K_1 and K_2 are known, in view of Eqs. **7** ($p_2 = \frac{1}{2}$) and **10a**, θ' can be calculated from

$$2\theta' = [K_1c'/(1 + K_1c')] + [K_2c'/(1 + K_2c')]. \quad [18]$$

This value may then be checked against the experimental curve (inflection region) for self-consistency. If necessary, both c' and θ' can be adjusted to achieve acceptable values.

The value of c' (above), together with K_1 and K_2, also can be used to calculate a value for the important parameter (see below) $L'(\rho) \equiv LY_{11}(\rho)/Y_{22}(\rho)$, from Eq. **17** (with $a = 1$):

$$L'(\rho) \equiv LY_{11}(\rho)/Y_{22}(\rho) = (1 + K_2c')^7/(1 + K_1c')^7. \quad [19]$$

When $K_2 \gg K_1$, c' is given approximately by $(L'^{1/7} - 1)/K_2$. The above procedure (c', θ', L') is used in the next section.

Whereas L (see above) is the equilibrium constant for $2 \rightleftarrows 1$ in isolated tropomyosin units, $L'(\rho)$ refers, per tropomyosin unit, to the process *all*-2 filament $\rightleftarrows$ *all*-1 filament, with Ca^{2+} at ρ, but in the absence of S-1. This follows from the fact that, in Eq. **17**, $L' = 1/a$ if $c = 0$. At low or high Ca^{2+}, we have the special cases

$$L'(0) = Lx_{11}/x_{22}\ (\rho \to 0);\ L'(\infty) = LK_a^2z_{11}/K_b^2z_{22}\ (\rho \to \infty). \quad [20]$$

When c is very large, because $K_2 \gg K_1$, in effect $a \to \infty$ and $p_2 \to 1$ (all state 2) in Eq. **12**. Thus, $\theta \to \theta_2$ (which allows evaluation of K_2—see below). Also, $p_{22} \to 1$ and $\sigma \to \sigma_{22}$. On the other hand, at $c = 0$, $a = 1/L'$ is small but not zero and p_2 is also small (largely state 1). From Eq. **12**, when a and a/Y are small (recall that $Y > 1$ for positive cooperativity),

$$p_2 = (a/Y)[1 + 2a - 3(a/Y) + \ldots]. \quad [21]$$

At $c = 0$ (S-1 absent), we put $a = 1/L'$ in this equation (ρ is arbitrary). Then $p_2 \cong 1/L'Y$ is a useful first approximation.

Special Case: No Interactions. In this case $x_{ij} = y_{ij} = z_{ij} = 1$. Note, in Eqs. **2**, that $Y = 1$ in this case but the separate $Y_{ij} \neq 1$ (unless $\rho = 0$). Then we find, as expected (2, 3),

$$\theta = p_1\theta_1 + p_2\theta_2,\ \sigma = p_1\sigma_1 + p_2\sigma_2 \quad [22]$$

$$p_1 = 1/(1 + a),\ p_2 = a/(1 + a) \quad [23]$$

$$\sigma_1 \equiv 2K_a\rho/(1 + K_a\rho),\ \sigma_2 \equiv 2K_b\rho/(1 + K_b\rho), \quad [24]$$

where

$$a = (1 + K_2c)^7(1 + K_b\rho)^2/L(1 + K_1c)^7(1 + K_a\rho)^2, \quad [25]$$

and θ_1 and θ_2 are given by Eq. **10**. This is a generalization of refs. 2 and 3 to include a second ligand (Ca^{2+}).

In the previous paper (1), Eq. **22a** (without the Ca^{2+} factors in Eq. **25**) was applied to the experimental data. The exponent 7 in Eq. **25** would have to be several times larger than 7 in order to achieve a reasonable fit of the ethylene glycol bis(β-aminoethyl ether)-*N,N,N',N'*-tetraacetic acid (EGTA) ($\rho = 0$) data. Eq. **22a** refers to a system with no neighbor interactions. The physical significance of increasing the exponent 7 in this way is that one is simulating, roughly, the actual attractive neighbor interactions by artificially forcing units to aggregate and to change state ($1 \rightleftarrows 2$) in small groups—but otherwise leaving neighbor interactions out of the model.

APPLICATION TO EXPERIMENTAL DATA

Experimental data are available (1) for $\theta(c)$, the S-1 binding isotherm, at, effectively, Ca^{2+} concentrations $\rho = 0$ and $\rho = \infty$ (actually, 1 mM EGTA and 0.5 mM $CaCl_2$). The experimental points are shown in Fig. 2. Our primary objective in this section is to attempt to fit these data with the above equations.

From six experimental points for both $\rho = 0$ and $\rho = \infty$ at $c \geq 1.8\ \mu M$, assuming $\theta = \theta_2$ in this region, we calculate the average value $K_2 = 7.1 \times 10^5\ M^{-1}$. The much smaller K_1 value presents more difficulty; we use $K_1 = 3 \times 10^3\ M^{-1}$. A smaller K_1, even $K_1 = 0$, has little effect on our fitting of the data. From the inflection in the $\rho = 0$ points, we estimate $c' = 1.15\ \mu M$. Eq. **18** then gives $\theta' = 0.226$ which, as can be seen from the figure, is certainly consistent with the data. We then find, from Eqs. **19** and **20**, $L'(0) = 63.7$. Turning to the $\rho = \infty$ points in Fig. 2, we estimate $c' = 0.46\ \mu M$. Then, from Eq. **18**, $\theta' = 0.124$, which is again clearly consistent with the data. Finally, from Eqs. **19** and **20**, $L'(\infty) = 7.16$. The ratio of these two L' values, for use below, is

$$L'(0)/L'(\infty) = K_b^2x_{11}z_{22}/K_a^2x_{22}z_{11} = 8.90. \quad [26]$$

The larger L' value (favoring state 1) in the absence of Ca^{2+} requires a larger value of c' (S-1) in order to induce the $1 \to 2$ transition, as is apparent in Fig. 2.

The above considerations are independent of the interaction parameter, Y. Of course Y is a function of ρ (Eqs. **2** and **6**) so we are concerned here with two values, $Y(0)$ and $Y(\infty)$. In either case, Y can be determined (approximately) by adjusting its value until the theoretical curve $\theta(c)$ appears to have the same slope as the experimental points in the neighborhood of $p_2 = \frac{1}{2}$ (i.e., at θ', c'). In the $\rho = 0$ case,

$$a = (1 + K_2c)^7/(1 + K_1c)^7L'(0),\ Y(0) = x_{11}x_{22}/x_{12}x_{21}. \quad [27]$$

If we assign a value to $Y(0)$ we have available (see above) all the parameters in Eqs. **27** needed in order to calculate $\theta(c)$ from Eqs. **7** and **12**. It is found that $\theta(c)$ with $Y(0) = 20$ reproduces the experimental slope at θ', c'; it also fits the remainder of the $\rho = 0$ points rather well. This is the lower solid-line curve in Fig. 2. The four points below the curve, near $c = 1\ \mu M$, are presumed to represent metastable rather than equilibrium behavior. Similarly, in the $\rho = \infty$ case,

$$a = (1 + K_2c)^7/(1 + K_1c)^7L'(\infty),\ Y(\infty) = z_{11}z_{22}/z_{12}z_{21}. \quad [28]$$

Again we have values for the parameters here, except $Y(\infty)$. Proceeding as above, we obtain the upper solid-line curve in Fig. 2, with $Y(\infty) = 4$. Note that there is stronger cooperativity in the *absence* of Ca^{2+} ($\rho = 0$).

Incidentally, the energetic significance of $Y(0) = 20$, for example, is the following. Since $x_{ij} = e^{-w_{ij}/kT}$ (see above), $Y(0) = e^{-w/kT}$, where

$$w \equiv w_{11} + w_{22} - w_{12} - w_{21}. \quad [29]$$

This is the free energy change for the rearrangement of two nearest-neighbor pairs, in the absence of Ca^{2+}, without any $1 \rightleftarrows 2$ conversion:

$$12 + 21 \to 11 + 22. \quad [30]$$

If w_{11} or w_{22} or both are negative, or if w_{12} or w_{21} or both are positive, or a combination of these, w will be negative and $Y(0) > 1$ (positive cooperativity), as in the above calculation. With $e^{-w/kT} = 20$, $w/kT = -3.0$; with $e^{-w/kT} = 4$, $w/kT = -1.4$.

The dotted curves in Fig. 2 show the calculated $p_2(c)$ in the two cases above ($\rho = 0, \infty$); this is the predicted fraction of tropomyosin units in state 2, as a function of c. At $c = 0$, the values are $p_2 = 0.00081$ for $\rho = 0$ and $p_2 = 0.041$ for $\rho = \infty$. These same values follow from Eq. **21**.

Intermediate Ca^{2+} Concentrations. Experiments are not yet available with finite Ca^{2+} concentrations, but we can use the above parameters (with some further assumptions) to make illustrative theoretical calculations for such cases.

What values should be used for the y_{ij}? If we assume, as seems reasonable in the absence of other information, that one bound Ca^{2+} has an effect on nearest-neighbor interactions that is intermediate between that of no bound Ca^{2+} (x_{ij}) and that of two bound Ca^{2+} (z_{ij}), then we may write $y_{ij} = (x_{ij}z_{ij})^{1/2}$. We use this relationship below. Two other (extreme) choices, not used here, are $y_{ij} = x_{ij}$ (the first bound Ca^{2+} has no effect on interactions) and $y_{ij} = z_{ij}$ (one bound Ca^{2+} has the same effect as two bound Ca^{2+}).

With the above "intermediate" assumption about y_{ij}, Y_{11} in Eq. 3 and σ_{11} in Eq. **11** become

$$Y_{11} = x_{11}[1 + K_a(z_{11}/x_{11})^{1/2}\rho]^2 \quad [31]$$

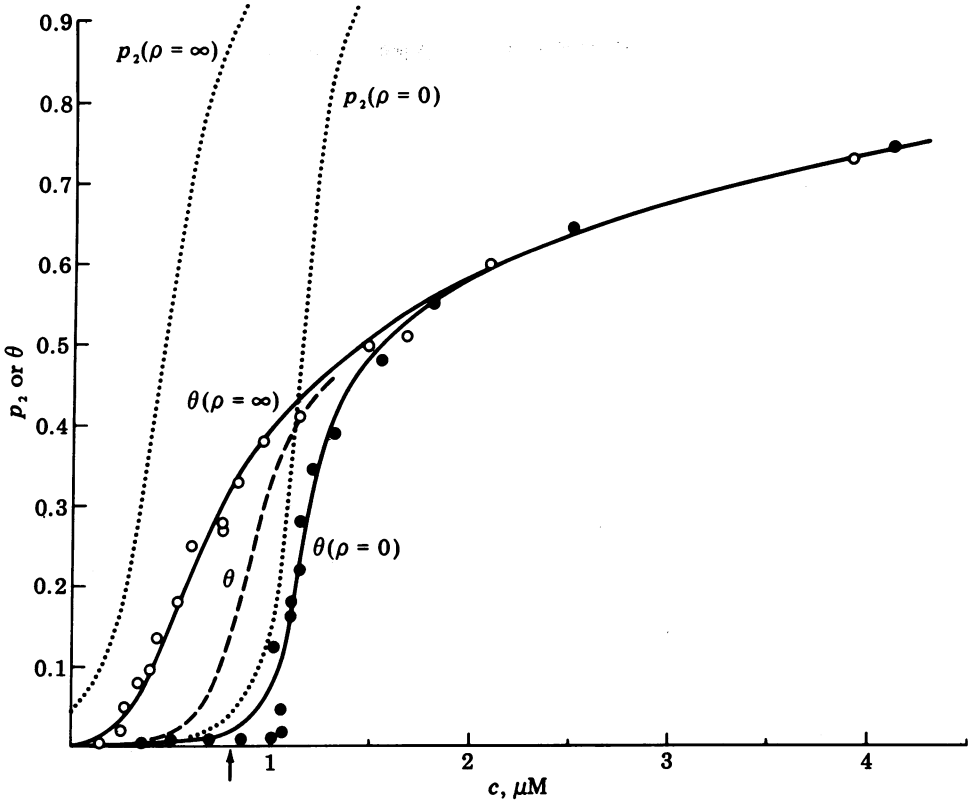

FIG. 2. The upper solid curve, $\theta(c)$ (S-1 binding), through experimental points O, is the theoretical curve at high Ca^{2+}. The lower solid curve with experimental points ●, is the corresponding low Ca^{2+} curve (EGTA, $\rho \cong 0$). The two dotted curves give the theoretical $p_2(c)$ behavior in the two cases. The dashed θ(c) curve has been calculated for $\rho = 0.15$ μM.

$$\sigma_{11} = 2K_a(z_{11}/x_{11})^{1/2}\rho/[1 + K_a(z_{11}/x_{11})^{1/2}\rho], \quad [32]$$

with similar expressions for the other Y_{ij} and σ_{ij}. The σ_{ij} are all simple Langmuir binding isotherms. If the actin binding sites are saturated with S-1 ($c \to \infty$), $p_{22} \to 1$ and the Ca^{2+} binding isotherm is $\sigma = \sigma_{22}$, with an effective binding constant of $K_b(z_{22}/x_{22})^{1/2}$. From the upper experimental curve in figure 2 of Bremel and Weber (13), which is very close to the Langmuir form, we estimate the above binding constant to be 7.9×10^6 M^{-1}. This value and Eq. 26 then determine $K_a(z_{11}/x_{11})^{1/2}$ (for σ_{11}) to be 2.65×10^6 M^{-1}, which is smaller by a factor of $\sqrt{8.90} = 2.98$. [Incidentally, from the lower Bremel and Weber curve, we estimate the latter (σ_{11}) binding constant to be 1.5×10^6 M^{-1}.]

We also need, in order to make calculations, $K_b(z_{12}/x_{12})^{1/2}$ and $K_a(z_{21}/x_{21})^{1/2}$. We *assume* (out of ignorance) that the ratio of these two constants is also 2.98. Their *product* is easily seen to be

$$7.9 \times 10^6 \times 2.65 \times 10^6 Y(0)^{1/2} Y(\infty)^{-1/2} = 4.68 \times 10^{13}\ M^{-2}.$$

Thus we find

$$K_b(z_{12}/x_{12})^{1/2} = 1.18 \times 10^7\ M^{-1},\ K_a(z_{21}/x_{21})^{1/2} = 3.96 \times 10^6\ M^{-1}.$$

We now have all the parameters needed for our sample calculations. The dashed curve in Fig. 2 shows $\theta(c)$ (S-1 binding) at a fixed free Ca^{2+} concentration of $\rho = 0.15$ μM. The value of Y (a constant) on this curve is 9.55. Also, along this curve, σ (Ca^{2+} binding) is 0.57 at $c = 0$, 0.82 at $c = 0.8$ μM, and 1.08 at $c = \infty$.

Although the equivalent experiment would be difficult, the central solid curve in Fig. 3 shows $\sigma(\rho)$ (Ca^{2+} binding) with free S-1 held constant at $c = 0.8$ μM (note the arrow in Fig. 2). Unlike Fig. 2, the cooperativity is not evident. Above this curve is the curve for $\sigma(\rho)$ when $c = \infty$ (i.e., $\sigma = \sigma_{22}$), and below it is the curve for $\sigma(\rho)$ when $c = 0$ (close to $\sigma = \sigma_{11}$). The dashed curve in Fig. 3 gives θ (S-1 binding) as a function of ρ (Ca^{2+}) in the $c = 0.8$ μM case.

CA^{2+} MODULATION OF S-1 BINDING CONSTANTS

So far we have assumed that K_1 and K_2 (for S-1 binding) are independent of the number of Ca^{2+} bound on a given tro-

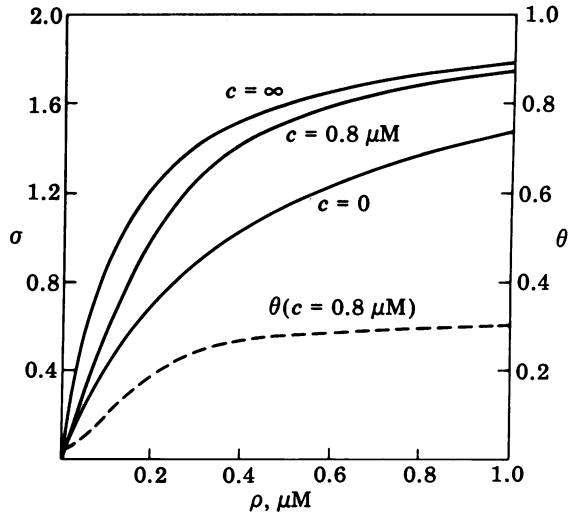

FIG. 3. The center solid curve is the calculated $\sigma(\rho)$ (Ca^{2+} binding) with $c = 0.8$ μM (note the arrow in Fig. 2); the upper and lower solid curves give $\sigma(\rho)$ for $c = \infty$ and $c = 0$, respectively. The dashed curve (right-hand scale) gives $\theta(\rho)$ (S-1 binding) in the $c = 0.8$ μM case.

pomyosin unit. The theory can still be carried out exactly with this restriction removed. We summarize the results here, in case they turn out to be useful in the future. We actually began this analysis with the appropriate (see below) 6 × 6 matrix of the type shown above, but we present the corresponding 2 × 2 matrix below for brevity.

K_1 (and similarly for K_2) is now replaced by three constants, K_{10}, K_{11}, and K_{12}, where 0, 1, 2 refer to the number of Ca^{2+} bound to a state 1 tropomyosin unit. We then introduce the grant partition functions

$$\xi_{1n} = L(1 + K_{1n}c)^7,\ \xi_{2n} = (1 + K_{2n}c)^7 \quad (n = 0,1,2) \quad [33]$$

$$\begin{aligned} a_1 &= \xi_{10}x_{11} + 2K_a\rho\xi_{11}y_{11} + K_a^2\rho^2\xi_{12}z_{11} \\ a_2 &= \xi_{20}x_{22} + 2K_b\rho\xi_{21}y_{22} + K_b^2\rho^2\xi_{22}z_{22} \end{aligned} \quad [34]$$

$$\begin{aligned} a_{12} &= \xi_{20}x_{12} + 2K_b\rho\xi_{21}y_{12} + K_b^2\rho^2\xi_{22}z_{12} \\ a_{21} &= \xi_{10}x_{21} + 2K_a\rho\xi_{11}y_{21} + K_a^2\rho^2\xi_{12}z_{21}. \end{aligned} \quad [35]$$

The fraction of actin sites occupied by S-1, on tropomyosin units in state j and with n Ca^{2+} bound is, from Eq. 33,

$$\theta_{jn} = K_{jn}c/(1 + K_{jn}c) \quad (j = 1,2;\ n = 0,1,2). \quad [36]$$

Let Θ_{ij} $(i,j = 1,2)$ be the average value of θ_{jn} on the *second member* (j) of a tropomyosin ij pair. Then it follows from Eqs. 34 and 35 that

$$\Theta_{11} = (\xi_{10}x_{11}\theta_{10} + 2K_a\rho\xi_{11}y_{11}\theta_{11} + K_a^2\rho^2\xi_{12}z_{11}\theta_{12})/a_1$$

$$\Theta_{22} = (\xi_{20}x_{22}\theta_{20} + 2K_b\rho\xi_{21}y_{22}\theta_{21} + K_b^2\rho^2\xi_{22}z_{22}\theta_{22})/a_2$$

$$\Theta_{12} = (\xi_{20}x_{12}\theta_{20} +)/a_{12},\ \Theta_{21} = (\xi_{10}x_{21}\theta_{10} +)/a_{21}, \quad [37]$$

where the omitted terms in the last line are obvious.

The 2 × 2 matrix for this problem is (compare Eq. 1)

$$\begin{pmatrix} a_1 & a_{12} \\ a_{21} & a_2 \end{pmatrix}. \quad [38]$$

(In the 6 × 6 matrix above, ξ_1 and ξ_2 in the six rows are replaced by ξ_{10}, ξ_{11}, ξ_{12}, ξ_{20}, ξ_{21}, ξ_{22}, respectively.) Eqs. 4, 5, and 12–16 all apply here but with $Y \equiv a_1a_2/a_{12}a_{21}$. The expression for θ is found to be

$$\theta = p_{11}\Theta_{11} + p_{22}\Theta_{22} + p_{12}(\Theta_{12} + \Theta_{21}), \quad [39]$$

while Eq. 8 gives σ, but with

$$\sigma_{11} = \partial\ln a_1/\partial\ln\rho = 2(K_a\rho\xi_{11}y_{11} + K_a^2\rho^2\xi_{12}z_{11})/a_1, \text{ etc.} \quad [40]$$

Whereas Eqs. 37 and 40 average over n (Ca^{2+}) for a given kind of tropomyosin pair, Eqs. 8 and 39 average further over the different pair types.

This model, and the simpler one above, both illustrate the great usefulness of and formal simplicity achieved by the introduction of subsystem grand partition functions (3), as in Eqs. 2, 3, and 33–35.

APPROXIMATE TREATMENT OF HMM BINDING

Returning now to the original model, suppose we are interested in *two-headed* HMM binding on actin (with no interactions between neighboring HMM molecules) instead of S-1 binding. This problem is difficult to treat exactly because of the possibility of HMM molecules binding at a tropomyosin 12 or 21 pair boundary, with one head attached to an actin site on either side of the boundary. However, an approximation can be obtained by applying functions derived for an infinite array of sites (11, 12) to the seven-site units. Thus, in place of Eqs. 3, we write (11, 12)

$$\begin{aligned} \xi_1 &= L\{[1 + (1 + 4K_1c)^{1/2}]/2\}^7 \\ \xi_2 &= \{[1 + (1 + 4K_2c)^{1/2}]/2\}^7, \end{aligned} \quad [41]$$

and, in place of Eqs. 10,

$$\theta_i = 4K_ic/[1 + (1 + 4K_ic)^{1/2}](1 + 4K_ic)^{1/2} \quad (i = 1,2). \quad [42]$$

Here, K_1, K_2, and c all refer to HMM rather than to S-1. No other changes are necessary. T. Tsuchiya and one of us (T.L.H.) will report on the exact solution to this problem.

1. Greene, L. & Eisenberg, E. (1980) *Proc. Natl. Acad. Sci. USA* **77**, 2616–2620.
2. Hill, T. L. (1952) *J. Chem. Phys.* **20**, 1259–1273.
3. Hill, T. L. (1960) *Introduction to Statistical Thermodynamics* (Addison-Wesley, Reading, MA).
4. Monod, J., Wyman, J. & Changeux, J. (1965) *J. Mol. Biol.* **12**, 88–118.
5. Hill, T. L. (1977) *Proc. Natl. Acad. Sci. USA* **74**, 3632–3636.
6. Hill, T. L. (1977) *Proc. Natl. Acad. Sci. USA* **74**, 4111–4115.
7. Hill, T. L. (1978) *Proc. Natl. Acad. Sci. USA* **75**, 1101–1105.
8. Hill, T. L. (1979) *Proc. Natl. Acad. Sci. USA* **76**, 714–716.
9. Hill, T. L. & Stein, L. (1980) *Proc. Natl. Acad. Sci. USA*, **77**, 693–697.
10. Hill, T. L. (1956) *Statistical Mechanics* (McGraw-Hill, New York), pp. 312–314, 323–324.
11. Hill, T. L. (1957) *J. Polymer Sci.* **23**, 549–562.
12. Hill, T. L. (1978) *Nature (London)* **274**, 825–826.
13. Bremel, R. D. & Weber, A. *Nature (London) New Biol.* **238**, 97–101.